Desalination and Water Treatment
www.deswater.com

doi: 10.5004/dwt.2018.22657

123 (2018) 41–51
August

The inactivation of fecal coliform using Fe_3O_4@Cu nanocomposite in real wastewater: emphasizing on synergic effect and inactivation mechanisms

Masoud Moradi[a], Ali Esrafili[b], Meghdad Pirsaheb[a], Vinod Kumar Gupta[c], Hooshmand Sharafi[d], Hossein Arfaeinia[e], Roshanak Rezaei Kalantary[b,f,*]

[a]*Research Center for Environmental Determinants of Health, Kermanshah University of Medical Sciences, Kermanshah, Iran, Tel. +989183855991; email: mahfooz60@gmail.com (M. Moradi), Tel. +989123446880; email: mpirsaheb@yahoo.com (M. Pirsaheb)*
[b]*Department of Environmental Health Engineering, School of Public Health, Iran University of Medical Sciences, Tehran, Iran, Tel. +98 9123234586; email: rezaei.k.r2016@gmail.com (R.R. Kalantary), Tel. +989124976672; email: A_esrafily@yahoo.com (A. Esrafili)*
[c]*Department of Applied Chemistry, University of Johannesburg, Johannesburg, South Africa, Tel. +27115596751; email: vinodfcy@gmail.com*
[d]*Student Research Committee, Kermanshah University of Medical Sciences, Kermanshah, Iran, Tel. +989183786151; email: Hooshmand.sharafi@gmail.com*
[e]*Department of Environmental Health Engineering, Faculty of Public Health, Bushehr University of Medical Sciences, Bushehr, Iran, Tel. +989178844836; email: Arfaeiniah@yahoo.com*
[f]*Research Center for Environmental Health Technology (RCEHT), Iran University of Medical Sciences, Tehran, Iran*

Received 12 January 2018; Accepted 21 June 2018

ABSTRACT

Fecal coliforms (FCs) are the main bacteriological indicators in the wastewater reuse. This study was conducted to evaluate the antimicrobial activity of Fe_3O_4@Cu nanocomposite for the FCs inactivation and to describe the inactivation mechanisms in real wastewater. Operational factors affecting the disinfectant process including pH, contact time, reagent dosage, wastewater quality, and synergic effect were studied. Results indicated iron has no synergic effect on antibacterial activity of copper but it can improve the toxicity of Cu. The inactivation of FCs until 40 min was corresponded to Cu^+ and Fe^{+2} ions. Increasing of total suspended solids (7–20 mg/L) and organic matter (13–24 mg/L) cause decreasing of antibacterial activity of Fe_3O_4@Cu up to 0.384 log, therefore, the inactivation of FCs in raw wastewater (RW) was less than activated sludge effluent (ASE). Increasing of reagent dosage up to 15 mg/L increased the FCs inactivation to 0.053 and 2.13 log for RW and ASE, respectively. The FCs inactivation was raised in acidic condition compared with natural and alkali conditions and specific lethality (Λ_{CW}) for Fe_3O_4@Cu nanocomposite was obtained 3.4 and 212 times more than those of Cu and Fe_3O_4. It can be concluded that the Fe_3O_4@Cu nanocomposite is effective antibacterial agent especially for ASE that can achieve WHO guideline and Iranian national standard limits.

Keywords: Fe_3O_4@Cu; Disinfection; Fecal coliform; Wastewater; Synergic effect

---

1. Introduction

Pathogen microorganisms in aquatic environment especially effluent of wastewater entail high risks for human health [1]. According to the World Health Organization, more than 80% of all diseases are caused by lack of access to world clean water [2]. Coliform bacteria are the main indicator of bacteriological water tests, which were introduced in 1914 by the American Public Health as an indicator of contamination of water [3]. Reuse of wastewater is the proper source for amends of water shortages in arid and semi-arid countries especially in agriculture field. Microbial risk is the serious problem in the reused wastewater [4,5]. Based on WHO guideline and Iranian standard, geometric mean of fecal coliforms (FCs) in secondary effluent of wastewater should not

---

* Corresponding author.

be exceeded from 1,000 and 400 MPN/100 mL, respectively [6]. For many years, different disinfectants including chlorine, chlorine dioxide, ozone, and Uv have been applied for water and wastewater disinfection [6]. Despite the effectiveness of these methods, wide range of disinfection by-products can be produced due to reaction of chemical disinfection with organic materials [7]. Accordingly, metal oxide nanomaterials are considered as new antibacterial agents [8]. Therefore, different metal and metal oxide nanoparticles such as Ag, Ag_2O, TiO_2, Si, CuO, ZnO, Au, CaO, and MgO have been applied as antibacterial agents [9]. Copper is more cost-effective over other metal oxide such as silver and shows relatively stable physical and chemical properties [10,11]. Moreover, copper has less toxicity than many metals on mammals but pose high toxicity on microorganisms which causes it to be applicable for inactivation of microorganisms [12]. Decorating surface of binary metal oxides using Cu was considered, which has performed to improve the antibacterial inactivation kinetics [13–16]. Since, the lack of nanocomposite separation causes secondary pollution of aquatic environments. Therefore, the wastewater disinfection with Cu decorated of Ag, ZnO, TiO_2, ZrO_2, Ce, polymers, etc. can be restricted due to increasing of nanoparticles in the effluent [17–19]. For this aim, applying paramagnetic iron oxide is an appropriate method to eliminate nanoparticles from aqueous solution by using external magnetic field [8]. On the other hand, combination of two nanoparticles is the suitable method to achieve a synergistic effect of them [20]. Recently, iron oxide nanoparticles have been emphasized for some noticeable applications in the field of antimicrobial activities [21]. Hence, this study was conducted to evaluate the antimicrobial activity of Fe_3O_4@Cu nanocomposite for the FCs inactivation and to describe the inactivation mechanisms in real wastewater.

2. Materials and methods

2.1. Wastewater sampling

Samples were taken from Iran University of Medical Sciences (IUMS) wastewater treatment plant (WWTP) from raw wastewater (RW) influent and activated sludge effluent (ASE). The WWTP was operated under extended aeration activated sludge process. Sampling strategy was based on daily gathering grab at 9 o'clock to achieve near same levels of microorganism concentration. Samples were collected by 1,000 mL vessels and transferred into the laboratory under the chain of custody [22]. The characterization of wastewater (RW and ASE) including chemical oxygen demand (COD), biological oxygen demand (BOD), pH, total suspended solids (TSS), metals (Cu and Fe), alkalinity, ammonium, temperature, and FC were determined according to standard methods for the examination of water and wastewater number 5,220, 5,210, 4,500, 2,540, 3,500, 2,320, 4,500, 2,550 and 9,221, respectively [23]. Composition of RW and ASE are showed in Table 1.

2.2. Reagents

All reagents were of analytical-laboratory grade, purchased from Merck®, Darmstadt, Germany, and used without further purification as follows: $FeCl_3 \cdot 6H_2O$ (CAS. 10025-77-1), $FeCl_2 \cdot 4H_2O$ (CAS. 13478-10-9), $NH_3 \cdot H_2O$, 25% (CAS. 1336-21-6), $CuSO_4 \cdot 5H_2O$ (CAS. 7758-99-8), A-1 medium (Catalogue Number 100415), borohydride ($NaBH_4$, 98%) (CAS. 16940-66-2), citric acid (CAS.77-92-9), and disodium phosphate (CAS. 7558-79-4).

2.3. Preparation of Fe_3O_4 nanoparticles

The Fe_3O_4 nanoparticles and Fe_3O_4@Cu nanocomposite were obtained by a coprecipitation method, which was suggested by Tang et al. and can be described briefly as follows. 6 mmol of $FeCl_2 \cdot 4H_2O$ and 10 mmol of $FeCl_3 \cdot 6H_2O$ were completely dissolved in deionized (DI) water under argon atmosphere, as a protective gas. 40 mL of 25% ammonia solution was diluted to reach 200 mL volume. Then, diluted ammonia was added into the above-mentioned Fe^{2+}/Fe^{3+} aqueous mixture dropwise and under vigorous mechanical agitation for 30 min at room temperature. Consequently, black sediment was obtained, and then was collected by applying an external magnetic field. The mixture was washed several times by DI water under 8,000 rpm centrifugation until obtaining neutral pH. Finally, the Fe_3O_4 nanoparticles were vacuum dried at 50°C [24].

2.4. Preparation of Fe_3O_4@Cu nanocomposites

First, 50 mg of Fe_3O_4 nanoparticles was dispersed in 50 mL of DI water, subsequently, 30 mL of $CuSO_4$ solution (0.2 mmol/L) was added to the mixture and sonicated for 30 min. Then, solution was strongly stirred for 30 min and

Table 1
Physicochemical and bacteriological characteristics of RW and ASE

Parameter	RW	RW + Fe_3O_4@Cu	ASE	ASE + Fe_3O_4@Cu
COD (mg/L)	480 ± 31	480 ± 31	27 ± 9	27 ± 9
BOD (mg/L)	288 ± 21	288 ± 21	7 ± 3	7 ± 3
pH	7.2 ± 0.25	7.2 ± 0.25	7.1 ± 0.12	7.1 ± 0.12
TSS (mg/L)	220 ± 40	220 ± 40	16 ± 8	16 ± 8
Cu (mg/L)	<0.02	0.64 ± 0.12	<0.02	0.78 ± 0.17
Fe (mg/L)	0.85 ± 0.12	1.1 ± 0.18	0.4 ± 0.2	1.35 ± 0.2
Alkalinity	712 ± 50	712 ± 50	520 ± 36	520 ± 36
NH_4-N	39 ± 2.4	39 ± 2.4	3.2 ± 0.8	3.2 ± 0.8
Temperature	27 ± 1.08	27 ± 1.08	27.6 ± 1.2	27.6 ± 1.2
FCs (MPN/100 mL)	8.5 ± 0.9E + 8		1.5 ± 0.68 E + 5	

then 0.6 g of $NaBH_4$ was quickly added and the mixture was allowed to react for 1 h under rapid stirring. The obtained Fe_3O_4@Cu was separated magnetically and washed several times with DI water to eliminate impurities. The product was then dispersed in10 mL of DI water [24].

2.5. Characterization

The analysis include X-ray diffraction (XRD) (model Shimadzu XRD-6000), using graphite monochromatic copper radiation (Cu Ka, $\lambda = 1.54$ Å) at 40 kV, 40 mA, and 25°C, scanning electron microscope (SEM) (model Philips XL30) at 15 keV, and Fourier transform infrared spectroscopy (FTIR) (Tensor 27, Bruker (Germany) spectrometer) in the range of 0–4,000 cm^{-1} were used to determine the diffraction pattern, surface morphology, and functional groups of Fe_3O_4@ Cu nanocomposite, respectively. Also, ICP-AES (inductively coupled plasma–atomic emission spectrometer) 7300 DV (USA) was used to determine the concentration of metal ions.

2.6. Disinfection assay of Fe_3O_4@Cu nanocomposite

Fe_3O_4@Cu ability for the inactivation of FCs under different levels of nanocomposite dosage (0.5–15 mg/L), pH (5, 7, and 9), contact time (0–60 min), TSS (7–20 mg/L), organic matter (13–24 mg/L), and initial number of FCs (10^5–10^8 MPN/100 mL) was studied. It is worth noting that other studies confirmed that range of bacteria concentration in effluent wastewater is similar to our result, For example, Rodríguez-González et al. [25] and Watts et al. [26] reported the total coliform bacteria present in the secondary effluent is 2.2×10^9 and 5×10^7 CFU/mL, respectively. Adjusting the pH values was conducted by using phosphate-citrate buffer solution. Experiments were conducted in 1 L model laboratory reactor. Nanocomposite was added into the reactor under 200 rpm stirring. Disinfectant activity was stopped by adding a mole-to-mole ratio of sodium thiosulfate as neutralizer and applying of external magnet for separation of the nanocomposite [6]. Supernatant was transferred into an A-1 medium to determine FCs using multiple-tube fermentation direct test according to APHA 2005 (method 9221 E). Subsequently, samples were immediately transferred to incubator with 35°C ± 0.5°C for 3 h, and then were placed in 44°C water bath for 21 ± 2 h [23]. Control experiments (without nanocomposite) and quantitative measurements of FCs were conducted in parallel of disinfection assay. In addition, synergic effect of nanoparticle was conducted through disinfection assay of Fe_3O_4 and Cu individually.

2.7. Metals ion release test

The release of copper and iron ions was conducted as follows: 0.1 g of Fe_3O_4@Cu nanocomposite was immersed in 6 mL 0.9% NaCl solution at 37°C for 24 h at pH = 7 [27]. To determine copper and iron ions release in actual condition, the same amount of Fe_3O_4@Cu nanocomposite was immersed in 10 mL of both the RW and ASE solutions. Before adding of nanocomposite, the existing copper and iron ions were measured in the RW and ASE solutions. For prevention of metal adsorption by solids, the TSS of solution was separated and then metals were determined in RW and ASE. Then the amount of Fe^{+2}, Fe^{+3}, Cu^{+}, and Cu^{+2} were measured with ICP-AES 7300 DV (detection limit of 0.005 mg/L) for description of disinfection mechanism [28].

2.8. Assessment of the synergic effect of Fe on Cu toxicity

The fractional inhibitory concentration (FIC) index was used in order to determine the combined effect of Cu and Fe as fallowing equation:

$$\frac{[\mathrm{Cu}]}{\mathrm{MIC}_{\mathrm{Cu}}} + \frac{[\mathrm{Fe}]}{\mathrm{MIC}_{\mathrm{Fe}}} = \mathrm{FIC}_{\mathrm{Cu}} + \mathrm{FIC}_{\mathrm{Fe}} = \sum \mathrm{FIC} \tag{1}$$

where [Cu] and [Fe] are concentrations of Cu and Fe ions, which exhibited the lowest inhibitory concentration. $\mathrm{MIC}_{\mathrm{Cu\ or\ Fe}}$ is the minimum concentration required to achieve complete inactivation by Cu ions (or Fe ions) alone. For this aim, the experimental assessment of MIC was conducted through microdilution method. The combination is considered synergistic, when the ΣFIC is ≤0.5; indifferent, when the ΣFIC is >0.5 to <2; and antagonistic, when the ΣFIC is ≥2 [29].

2.9. The evaluation of disinfection kinetics

Because of the complicated nature of disinfection process, to simplify the mechanisms, five assumptions were considered for kinetic inactivation models in batch reactors as follows: (1) uniform spreading of organisms and disinfectant molecules; (2) adequate mixing to provide proper liquid diffusion; (3) back mixing was not occurred; (4) temperature and pH are fixed; (5) the disinfectant concentration remains constant during the contact time [30]. Based on Chick's Law, disinfection model obeyed pseudo-first-order reaction assigned to the organism's concentration [31].

$$r = -k_c N \tag{2}$$

where r is reaction rate for the decrease in viable organisms with time (org/L min), k_c is Chick's law rate constant (min^{-1}), and N is assigned to concentration of organisms (org/L).

In addition, Watson suggested that the time necessary to reach a specific level of disinfection was related to the disinfectant concentration by the following equation:

$$C^n t = \text{Constant} \tag{3}$$

where C = concentration of disinfectant (mg/L); n = empirical constant related to concentration (unitless); t = time required to achieve a constant percentage of inactivation (e.g., 99%); Constant = value for given percentage of inactivation (dimensionless).

With respect to that, disinfection concentration and time are of equal importance, Chick's law and the Watson equation can be combined as follows:

$$r = -\Lambda_{\mathrm{CW}} C N \tag{4}$$

$$\ln \frac{N_t}{N_0} = -\Lambda_{\mathrm{CW}} C t \tag{5}$$

where Λ_{CW} is coefficient of specific lethality (disinfection rate constant) (L/mg min), N_0 is concentration of organisms at time = 0 (org/L), and t = time (min).

3. Results and discussion

3.1. Characterization of the Fe_3O_4@Cu nanocomposite

FTIR spectra were recorded on a Tensor 27, Bruker (Germany) spectrometer. Fig. 1 shows an obvious adsorption bond at 565.3 cm^{-1}, which is attributed to Fe–O vibration due to Fe_3O_4 [32], another peak at 1,220.24 cm^{-1} can be corresponded to C–N bond stretching, the peaks at 1,812.68, 3,164.61, and 3,693.38 cm^{-1} can be assigned to C=O, C–H, and O–H stretching vibrations, respectively [24]. Fig. 2 shows the EDX analysis applying to ensure the presence of elements such as copper, oxygen, and iron in the synthesized composite structure. The peaks for iron also prove the existence of Fe on the Fe_3O_4@Cu nanocomposite surface. The analysis also revealed the elements percent (w/w) obtained 2.44%, 63.79%, and 33.76% in the nanocomposite structure for copper, oxygen, and iron, respectively. These results suggested that the majority of nanocomposite surface was occupied by oxygen in the form of Fe_3O_4 and CuO particles.

Phase and crystal structure of Fe_3O_4@Cu nanocomposite and Fe_3O_4 nanoparticles were recognized by applying XRD which can be shown in Fig. 3. The pattern of the nanocomposite shows that the seven peaks at 2θ = 18.27°, 30.1°, 35.4°, 43.05°, 56.94°, 62.5°, and 73.95°correspond to the diffraction of (111), (220), (311), (400), (422), (511), and (533) are consistent with the standard XRD data for cubic crystalline structures of Fe_3O_4 [33]. Whereas, an additional peak at 50.40° from the (200) lattice plane of the metallic Cu nanoparticles was observed for Fe_3O_4@Cu. The metal Cu nanoparticles peaks at 43.3° and 73.99° are overlapped with the 43.2° and 74.3° peaks of Fe_3O_4 [24,33]. Fig. 4 shows the SEM image of Fe_3O_4 nanoparticles and Fe_3O_4@Cu nanocomposite at 15 keV. SEM image shows the Fe_3O_4@Cu nanocomposite has polycrystalline pattern and particles have been greatly agglomerated.

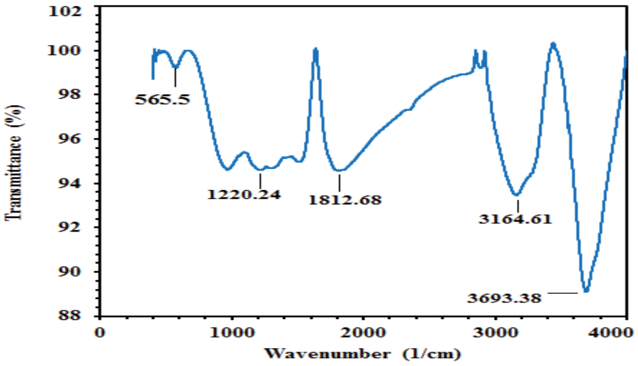

Fig. 1. The FTIR spectra of Fe_3O_4@Cu nanocomposite.

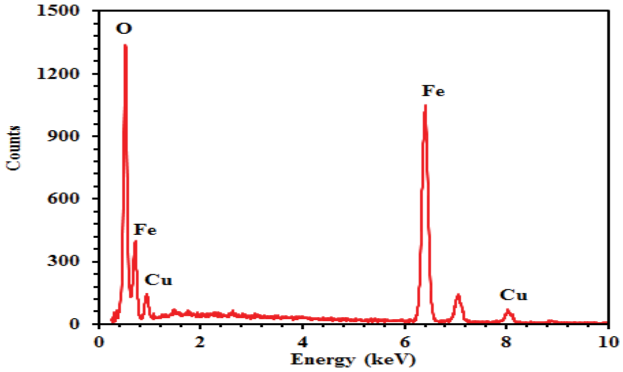

Fig. 2. The EDX patterns of Fe_3O_4@Cu.

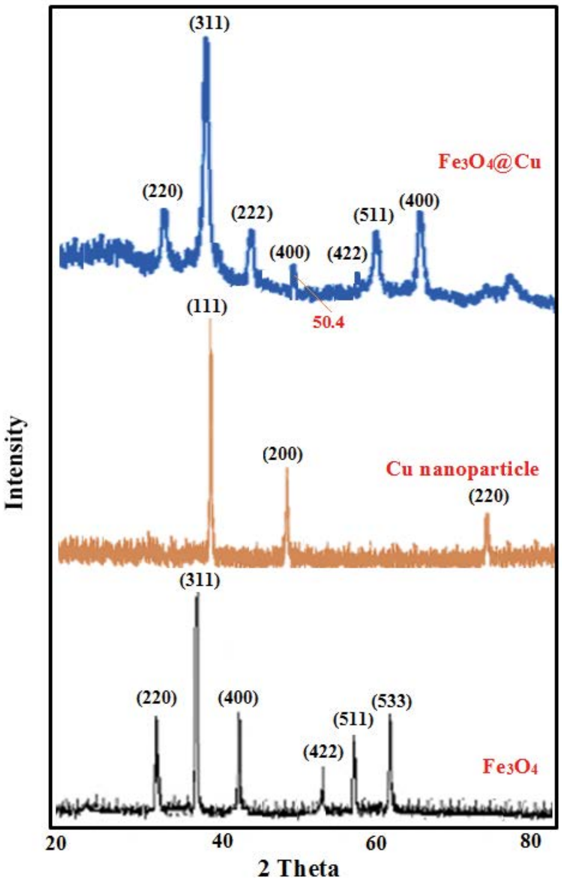

Fig. 3. The XRD patterns of Fe_3O_4, Cu nanoparticle, and Fe_3O_4@Cu.

3.2. Copper and iron ions release

The concentration of copper and iron ions after 3 d of immersion is shown in Table 2. Results indicated that, copper and iron releasing into NaCl (0.9%), RW and ASE solutions were 8.4 × 10^{-3} and 1.5 × 10^{-2} mg/g, 7 × 10^{-2} and 1 × 10^{-2} mg/g, and 9 × 10^{-3} and 12.3 × 10^{-2} mg/g, respectively. Results showed that releasing of copper was less than those of iron and their order in solutions were obtained as follows: ASE > RW > 0.9% NaCl.

3.3. Description of antibacterial mechanism of Fe_3O_4@Cu nanocomposite

The antibacterial mechanism of copper nanoparticles has been attributed to the fact that copper ions leaching from

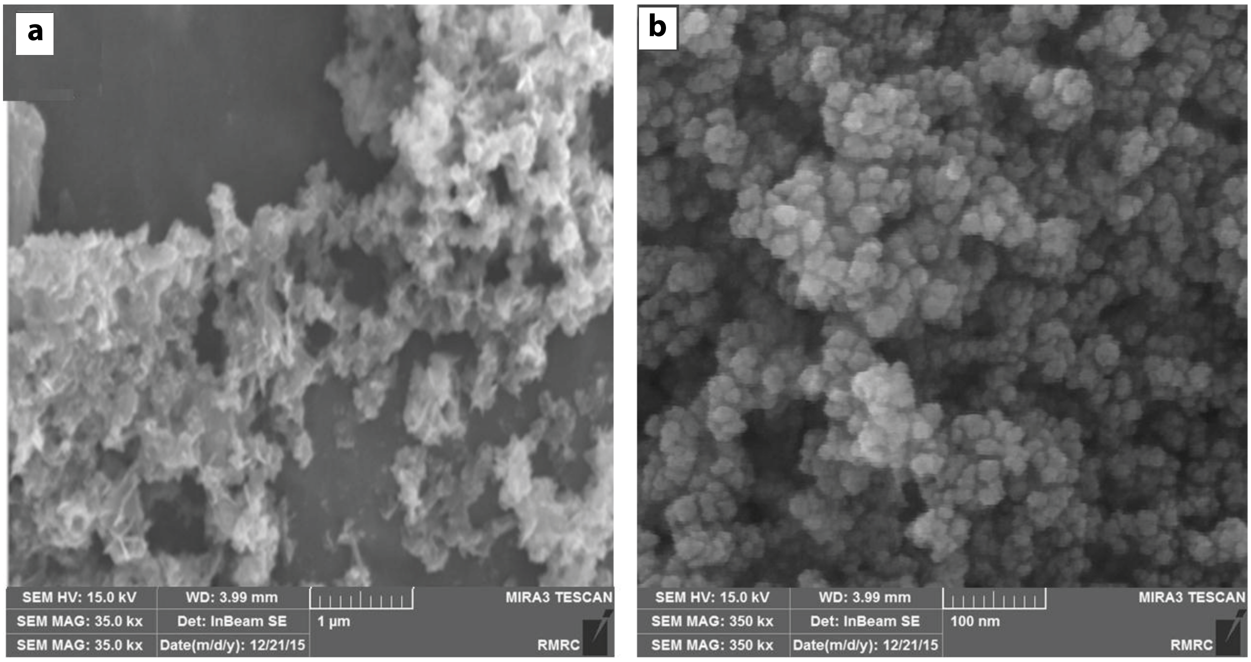

Fig. 4. The SEM image of Fe_3O_4 (a) and Fe_3O_4@Cu (b).

Table 2
Cu and Fe ions concentration and release rate in 0.9% NaCl, RW and ASE solutions

Parameters	0.9% NaCl solution	RW	ASE
Fe_3O_4@Cu nanocomposite (g/L)	16	10	10
Cu concentration (mg/L)	0.14 ± 0.08	0.7 ± 0.13	0.9 ± 0.15
Fe concentration (mg/L)	0.25 ± 0.11	1 ± 0.12	1.23 ± 0.18
mg Cu release per gram nanocomposite	8.4×10^{-3}	7×10^{-2}	9×10^{-2}
mg Fe release per gram nanocomposite	1.56×10^{-2}	1×10^{-2}	12.3×10^{-2}

nanoparticles are absorbed by bacteria [34]. Figs. 5 and 6 reveal that the inactivation of FCs until 40 min corresponded to Cu^+ and Fe^{+2}. Also, the Cu (I) and Fe(II) were converted to Cu(II) and Fe(III) by increase of time. Two species oxidized of copper include cupric (Cu^{+2}), and reduced cuprous (Cu^+), can be existed in solution [35]. Leaching of Cu complexes from Fe_3O_4@Cu nanocomposite by bacterial amino acids is required for their antimicrobial toxicity [36]. Cu^+ is significantly more toxic to bacteria than Cu^{2+} due to membrane permeability [37]. Hence, Cu^+ interferes with cell wall synthesis and cell division, and may alter the ratio of some macromolecular ingredients [38]. On the other hand, surface negative of FCs and positive charges of copper ions cause adhesion and bioactivity of ions to bacteria via electrostatic forces [39]. Also, Fe^{2+} released from nanocomposite into the water body causes the FCs inactivation to produce reactive radicals [40].

3.4. Effect of the exposure time on FCs inactivation

Fig. 7 shows the exposure time of FCs with nanocomposite. As observed, the inactivation of FCs in RW and ASE during exposure time was different. Results revealed that after 60 min, 8 mg/L of Fe_3O_4@Cu can reduce of FCs between 0.019 and 0.788 log (4.2% and 84%) for RW and ASE, respectively. Nevertheless, the inactivation of FCs has not significantly changed by increasing the time ($P > 0.05$). Ochoa-Herrera et al. [41] reported that the concentration of the toxicant was decreased considerably with time which probably was due to the attenuation of soluble copper or microbial adaptation. On the other hand, the study of Domek [42] showed the progressive injury greater than 90% and 99.5% of *Escherichia coli* cells caused by exposure to 0.05 mg/L copper in inorganic carbon buffer within 2 and 5 d at 4°C, respectively.

3.5. Effect of reagent dosage on FCs inactivation

Fig. 8 shows the effect of nanocomposite dosage on FCs inactivation in RW and ASE. As indicated, by increasing the nanocomposite dosage from 0.5 to 15 mg/L, the FCs inactivated were obtained 0.053 and 2.13 log (11.4% and 99.25%) for RW and ASE, respectively. Results revealed that achieve to standards of WHO and Iranian national for ASE was possible by using the 8 and 15 mg/L of nanocomposite, respectively (Fig. 9). Low inactivation of FCs in RW can be attributed to the protective effect of suspended solids and organic matter for microorganisms against the effect of copper [43].

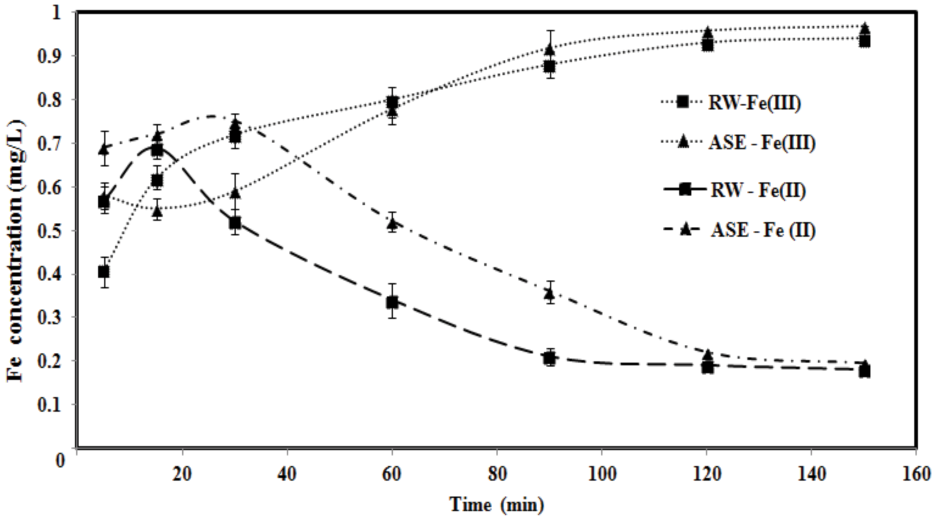

Fig. 5. The release of iron from Fe_3O_4@Cu nanocomposite for RW and ASE (exposure time = 150 min, TSS = 12 ± 1.4, SCOD = 20 ± 2.6).

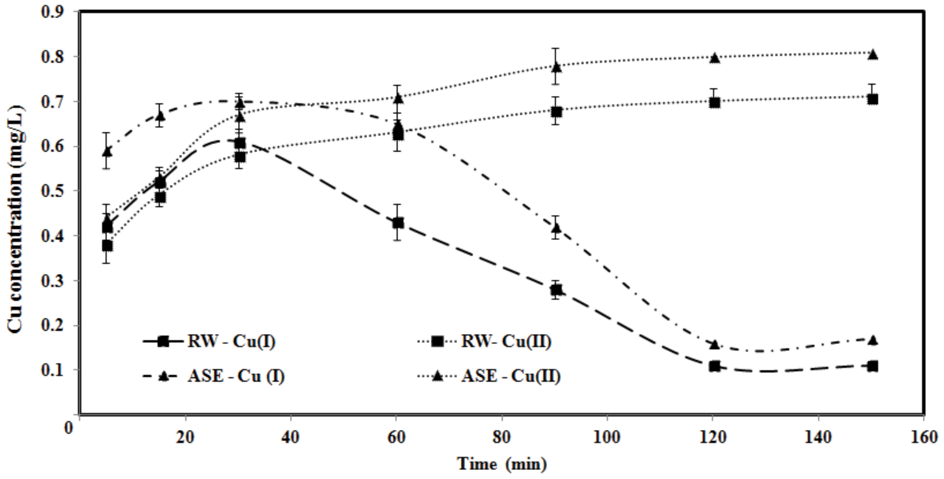

Fig. 6. The release of Cu from Fe_3O_4@Cu nanocomposite for RW and ASE (exposure time = 150 min, TSS = 12 ± 1.4, SCOD = 20 ± 2.6).

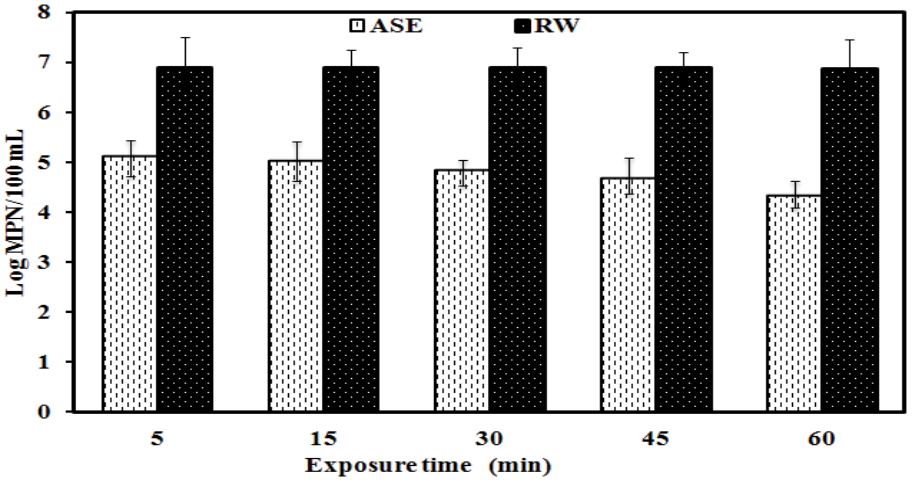

Fig. 7. The effect of exposure time on fecal coliform inactivation using Fe_3O_4@Cu disinfectant (pH = 7, TSS = 15 ± 3, SCOD = 24 ± 4, log initial MPN (ASE = 5.176 ± 0.021, RW = 6.903 ± 0.032 MPN/100 mL)).

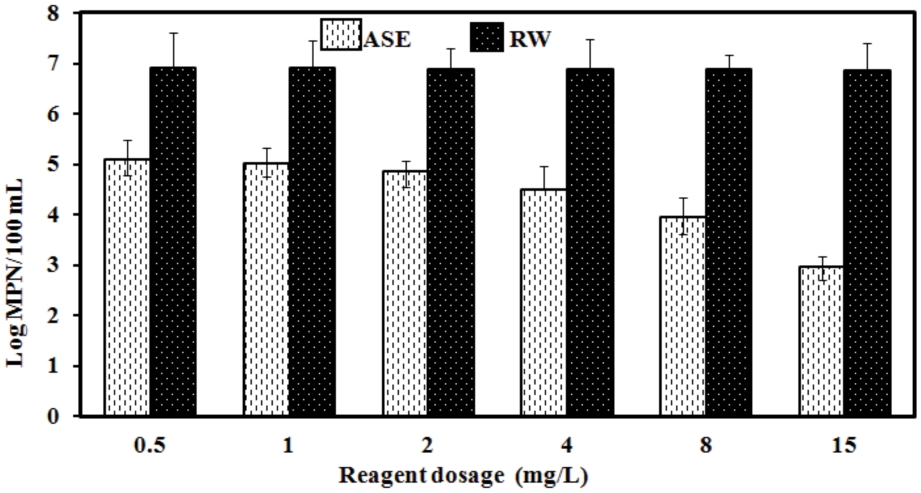

Fig. 8. The effect of reagent dosage on inactivation of fecal coliform (pH = 7, exposure time = 60 min, TSS = 16 ± 4, SCOD = 25 ± 6.2, log initial MPN (ASE = 5.13 ± 0.018, RW = 6.87 ± 0.028 MPN/100 mL)).

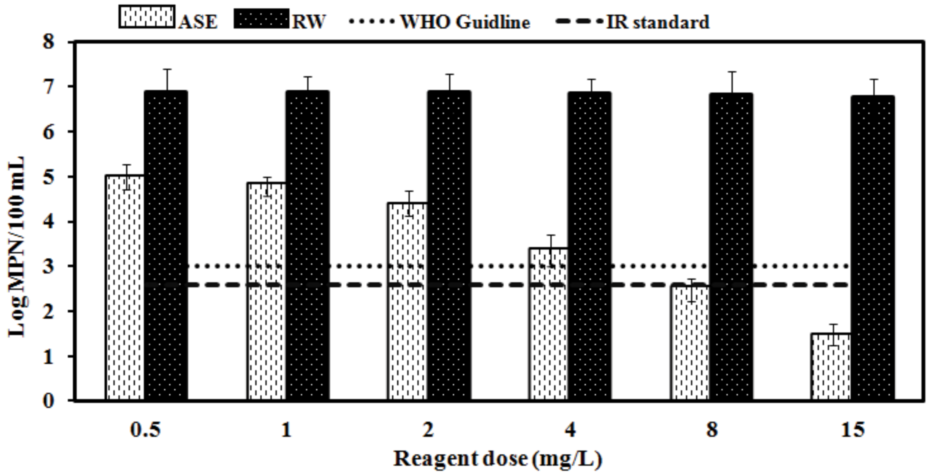

Fig. 9. The inactivation of fecal coliform using Fe_3O_4@Cu compared with WHO and IR standard (pH = 7, exposure time = 60 min, TSS = 18 ± 4.5, SCOD = 27 ± 5.2, log initial MPN (ASE = 5.22 ± 0.047, RW = 7 ± 0.072 MPN/100 mL)).

Ochoa-Herrera et al. [41] indicated that 10 mg/L of copper(II) have a moderate stimulatory effect on the microbial oxidation of ammonia to nitrate. Kurmaç [44] indicated that 10–50 mg/L of copper has antimicrobial effect via inhibition of respiration and microbial growth.

3.6. Synergic effect of iron on antibacterial activity of copper

The synergic effect of iron is shown in Table 3. Results showed that maximum inactivation of FCs by copper and iron (15 mg/L) in ASE obtained 1.073 and 0.038 log (91.54% and 8.4%), respectively, while for combination of two metals (Fe_3O_4@Cu), it obtained 3.79 log (99.98%) (Fig. 10). As results indicated, the iron has no synergic effect on antibacterial activity of copper in terms of FCs inactivation (∑FIC > 0.5). But this study indicated that iron has remarkable effect on antibacterial activity of copper. Because iron facilitates the separation of nanocomposite (prevents the secondary contamination of nanocomposite), improves the toxicity of copper via reduction of Cu^{2+} to Cu^{+} and production of reactive oxygen species [45]. Moreover, iron contributes to the inactivation process through intermediate S radical chemistry in bacteria cell [46].

Table 3
Synergic effect of iron on antibacterial activity of copper

MIC			FIC Cu	FIC Fe	∑FIC
Cu (mg/L)	Fe (mg/L)	Fe_3O_4@Cu			
7	20	4	0.57	0.2	0.77

3.7. The evaluation of disinfection kinetics

Fig. 11 shows the disinfection kinetic by Fe_3O_4@Cu nanocomposite. The slope of the line in the plot corresponds to the coefficient of specific lethality (Λ_{CW}). Result revealed the Λ_{CW}

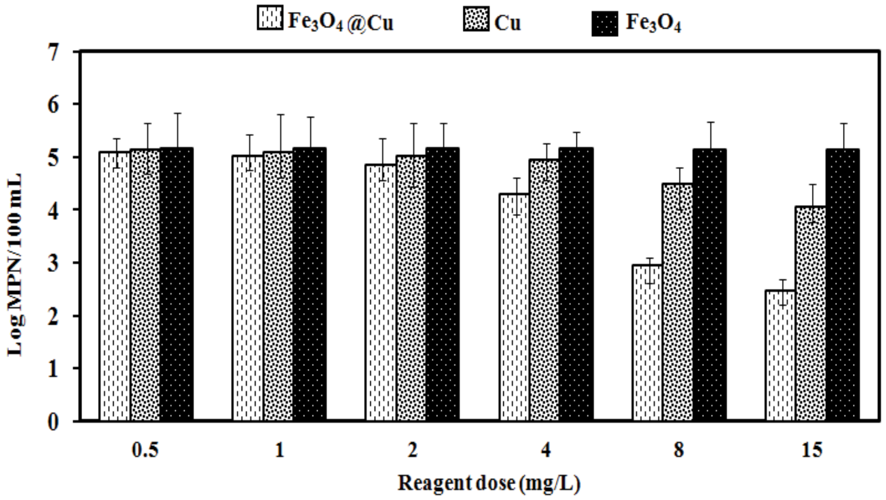

Fig. 10. The synergic effect of Fe on Cu toxicity (pH = 7, exposure time = 60 min, TSS = 14 ± 3.4, SCOD = 22 ± 3.8, log initial MPN (ASE = 5.16 ± 0.014 MPN/100 mL)).

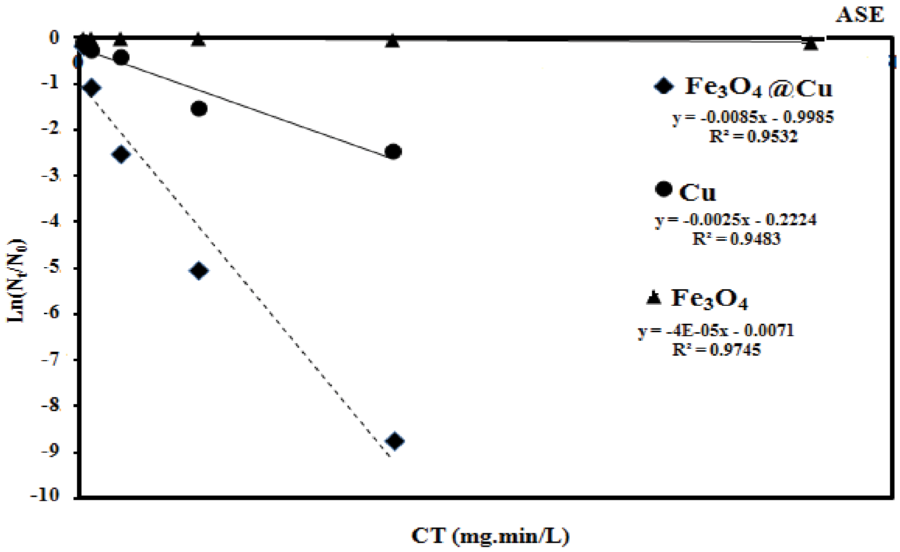

Fig. 11. Linear fitting plots of disinfection kinetics according to Chick–Watson model (pH = 7, exposure time = 60 min, TSS = 13 ± 2.5, SCOD = 20 ± 3.6, log initial MPN (ASE = 5.04 ± 0.012 MPN/100 mL)).

for Fe_3O_4@Cu nanocomposite is 3.4 and 212 times more than those of Cu and Fe_3O_4, respectively. Increasing the specific lethality (Λ_{CW}) explains the high ability of disinfectant for inactivation of bacteria [47]. Kim [48] indicated the coefficients of specific lethality were increased by increasing oxidation potentials of disinfectants. De la Rosa-Gómez [49] reported that coefficients of specific lethality of Ag-OZ were more than Ag-SZ for inactivation of *E. coli* from wastewater-like.

3.8. Effect of wastewater quality

3.8.1. Effect of TSS and organic matter

Fig. 12 shows the effect of TSS and soluble COD (SCOD) concentration on antibacterial activity of Fe_3O_4@Cu nanocomposite. Results indicated with increasing of TSS concentration (7–20 mg/L) and SCOD (13–24 mg/L), the FCs inactivation decreased from 0.576 to 0.192 log (73.45%–35.73%) in ASE. Results showed TSS and SCOD are the important parameters that affected on antibacterial activity of copper through decreasing of the availability and toxicity of copper ions to FCs [42]. Suspended particles scavenge the copper and iron ions through adsorption and precipitation reactions that lead to considerable decreasing of FCs inactivation [41,50]. Pamukoglu [51] showed the increasing of biomass causing reduction of copper toxicity. Regarding this, the suspended particles act as shield for the microorganisms and protect them against disinfectants. For this reason, the disinfectant becomes less effective in RW than ASE [52]. Organic matter is also the important parameter that affected on antibacterial activity of copper by complexation with free Cu^+/Cu^{2+} and formation of low soluble copper ions [53,54]. Daly et al. [55]

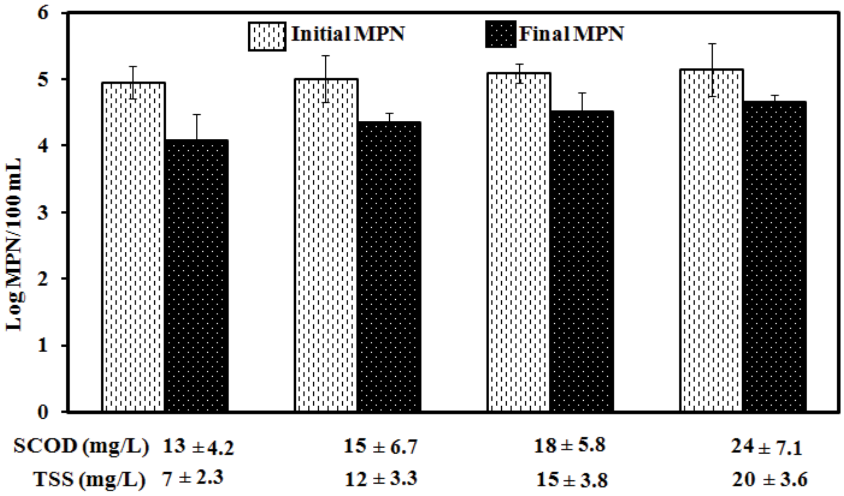

Fig. 12. The effect of TSS and SCOD on antibacterial activity of Fe_3O_4@Cu disinfectant (pH = 7, reagent dose = 8 mg/L, exposure time = 60 min, log initial MPN = 4.954–5.146 MPN/100 mL).

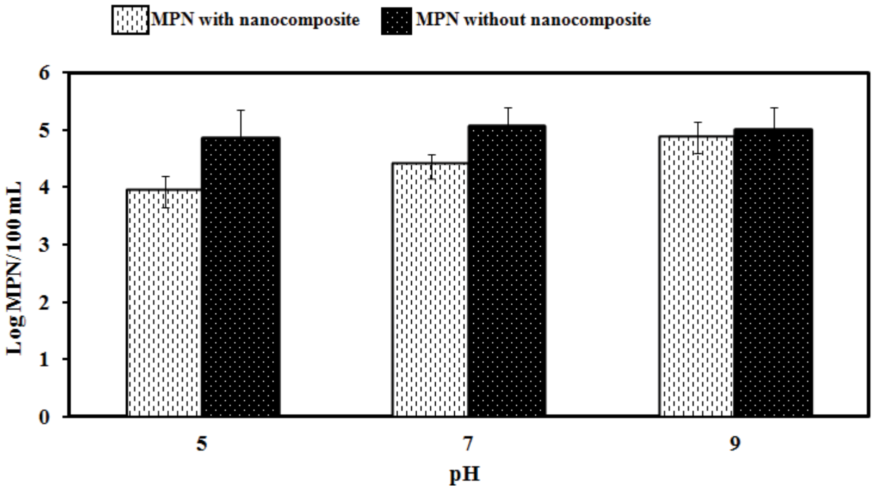

Fig. 13. The effect of pH on inactivation of fecal coliform using Fe_3O_4@Cu disinfectant (exposure time = 60 min, TSS = 16 ± 3.4, SCOD = 23 ± 4.6, log initial MPN (ASE = 5.079 ± 0.018 MPN/100 mL)).

showed the toxicity of copper on *Paratya australiensis* was significantly reduced by increasing natural organic matter.

3.9. Effect of pH

pH is the main parameter that affected the efficiency of nanocomposite [56]. Fig. 13 shows the effect of different pH on FCs inactivation. Result showed the inactivation of FCs at acidic, natural, and alkali (5, 7, and 9, respectively) without applying nanocomposite was obtained as 40%, 1%, and 16.6%, respectively. While, the inactivation of FCs using Fe_3O_4@Cu nanocomposite was increased to 92.5%, 77.5%, and 35% at acidic, natural, and alkali, respectively. Results indicated the inactivation of FCs in the acidic condition (pH = 5) is more than those obtained from natural and alkali conditions. Changing of pH value from 7 to 5 stimulates FCs (especially *E. coli*) to synthesize cyclopropane fatty acids. This phenomenon reduces H^+ ion permeability influx and increases its efflux [57]. Moreover, the Fe^{+2} and Cu^{+2} is more released at the acidic condition, which improved the inactivation of FCs [58]. While, the inactivation of FCs was decreased at alkali condition due to formation of hydroxide form of metals [59]. The following reactions are related to release copper from nanocomposite at alkali condition [58]:

$$2Cu^{+} + 2OH^{-} \rightarrow Cu_2O + H_2O + 2e^{-} \tag{6}$$

$$Cu_2O + 2OH^{-} + H_2O \rightarrow 2Cu(OH)_2 + 2e^{-} \tag{7}$$

4. Conclusion

It can be concluded that FCs are the main bacteriological indicators in the wastewater reuse. Metal nanoparticles are considered as antibacterial agents and copper over other metal is cost advantage and relatively stable physical–chemical properties and less toxic than many metals to mammals but highly toxic to microorganisms. This study revealed that the inactivation of FCs until 40 min corresponded to Cu^+ and Fe^{+2}. Also, achieve to standards of WHO and Iranian national standard for ASE was possible by using the 8 and 15 mg/L of nanocomposite, respectively. Results indicated iron has no synergic effect on antibacterial activity of copper but it can improve Cu toxicity. The inactivation of FCs was increased in acidic condition due to more release of metals ions. Moreover, increasing of TSS and organic matter causes decrease of antibacterial activity of Fe_3O_4@Cu, therefore, the inactivation of FCs in RW was less than ASE. It can be concluded that the Fe_3O_4@Cu nanocomposite is effective antibacterial agent especially for ASE that can achieve WHO guideline and Iranian national standard limits.

Acknowledgment

The authors wish to warmly acknowledge the invaluable cooperation and support from the Deputy and Chemistry laboratory staff of Iran University of Medical Sciences for facilitating the issue of this project.

References

[1] K. Sharafi, M. Moradi, A. Karami, T. Khosravi, Comparison of the efficiency of extended aeration activated sludge system and stabilization ponds in real scale in the removal of protozoan cysts and parasite ova from domestic wastewater using Bailenger method: a case study, Kermanshah, Iran, Desal. Wat. Treat., 55 (2015) 1135–1141.

[2] N. Mirzaei, H. Ghaffari, K. Karimyan, F. Moghadam, A. Javid, K. Sharafi, Survey of effective parameters (water sources, seasonal variation and residual chlorine) on presence of thermotolerant coliforms bacteria in different drinking water resources, Int. J. Pharm. Technol., 7 (2015) 9680.

[3] K. Sharafi, M. Pirsaheb, T. Khosravi, A. Dargahi, M. Moradi, M. Savadpour, Fluctuation of organic substances, solids, protozoan cysts, and parasite egg at different units of a wastewater integrated stabilization pond (full scale treatment plant): a case study, Iran, Desal. Wat. Treat., 57 (2016) 4913.

[4] H. Biglari, M. Afsharnia, V. Alipour, R. Khosravi, K. Sharafi, A.H. Mahvi, A review and investigation of the effect of nanophotocatalytic ozonation process for phenolic compound removal from real effluent of pulp and paper industry, Environ. Sci. Pollut. Res., 24 (2017) 4105–4116.

[5] K. Sharafi, M. Pirsaheb, R. Davoodi, H.R. Ghaffari, M. Fazlzadeh, M. Karimaei, M. Miri, K. Dindarloo, A. Azari, H. Arfaeinia, Quantitative microbial risk assessment of *Giardia* cyst and *Ascaris* egg in effluent of wastewater treatment plants used for agriculture irrigation – a case study, Desal. Wat. Treat., 80 (2017) 142.

[6] K. Sharafi, M. Fazlzadeh, M. Pirsaheb, M. Moradi, A. Azari, H. Sharafi, K. Dindarloo, H.R. Ghafari, Wastewater disinfection using sodium dichloroisocyanate (NaDCC) and sodium hypochlorite (NaOCL): modeling, optimization and comparative analysis, Desal. Wat. Treat., 66 (2017) 221–228.

[7] M.H. Habibollahi, A. Baghizadeh, A. Sabokbara, K. Sharafi, Isolation and characterization of copper and cadmium resistant bacteria from industrial wastewaters and evaluating the biosorption of selected bacteria, Desal. Wat. Treat., 93 (2017) 139–144.

[8] A. Sheikhmohammadi, Z. Dahaghin, S.M. Mohseni, M. Sarkhosh, H. Azarpira, Z. Atafar, M. Abtahi, S. Rezaei, M. Sardar, H. Masoudi, M. Faraji, The synthesis and application of the SiO_2@ Fe_3O_4@ MBT nanocomposite as a new magnetic sorbent for the adsorption of arsenate from aqueous solutions: modeling, optimization, and adsorption studies, J. Mol. Liq., 255 (2018) 313–323.

[9] S.M. Dizaj, F. Lotfipour, M. Barzegar-Jalali, M.H. Zarrintan, K. Adibkia, Antimicrobial activity of the metals and metal oxide nanoparticles, Mater. Sci. Eng., C, 44 (2014) 278.

[10] A. Ananth, S. Dharaneedharan, M.-S. Heo, Y.S. Mok, Copper oxide nanomaterials: synthesis, characterization and structure-specific antibacterial performance, Chem. Eng. J., 262 (2015) 179.

[11] M. Moradi, A.M. Mansouri, N. Azizi, J. Amini, K. Karimi, K. Sharafi, Adsorptive removal of phenol from aqueous solutions by copper (cu)-modified scoria powder: process modeling and kinetic evaluation, Desal. Wat. Treat., 57 (2016) 11820–11834.

[12] N.M. Zain, A. Stapley, G. Shama, Green synthesis of silver and copper nanoparticles using ascorbic acid and chitosan for antimicrobial applications, Carbohydr. Polym., 112 (2014) 195.

[13] S. Rtimi, S. Giannakis, R. Sanjines, C. Pulgarin, M. Bensimon, J. Kiwi, Insight on the photocatalytic bacterial inactivation by co-sputtered TiO_2–Cu in aerobic and anaerobic conditions, Appl. Catal., B, 182 (2016) 277.

[14] H. Ishiguro, Y. Yao, R. Nakano, M. Hara, K. Sunada, K. Hashimoto, Y. Kubota. Photocatalytic activity of Cu^{2+}/TiO_2-coated cordierite foam inactivates bacteriophages and *Legionella pneumophila*, Appl. Catal., B, 129 (2013) 56–61.

[15] P. Bleichert, C.E. Santo, M. Hanczaruk, H. Meyer, G. Grass, Inactivation of bacterial and viral biothreat agents on metallic copper surfaces, Biometals, 27 (2014) 1179–1189.

[16] O. Baghriche, S. Rtimi, C. Pulgarin, R. Sanjines, J. Kiwi, Effect of the spectral properties of TiO_2, Cu, TiO_2/Cu sputtered films on the bacterial inactivation under low intensity actinic light, J. Photochem. Photobiol., A, 251 (2013) 50–56.

[17] P.M. Linnik, I.B. Zubenko, Role of bottom sediments in the secondary pollution of aquatic environments by heavy-metal compounds, Lake Reservoirs Res. Manage., 5 (2000) 11–21.

[18] P. Biswas, R. Bandyopadhyaya, Synergistic antibacterial activity of a combination of silver and copper nanoparticle impregnated activated carbon for water disinfection, Environ. Sci. Nano, 4 (2017) 2405–2417.

[19] L. Tamayo, M. Azócar, M. Kogan, A. Riveros, M. Páez. Copper-polymer nanocomposites: an excellent and cost-effective biocide for use on antibacterial surfaces, Mater. Sci. Eng., C, 69 (2016) 1391–1409.

[20] J.P. Ruparelia, A.K. Chatterjee, S.P. Duttagupta, S. Mukherji, Strain specificity in antimicrobial activity of silver and copper nanoparticles, Acta Biomater., 4 (2008) 707–716.

[21] S.S. Behera, J.K. Patra, K. Pramanik, N. Panda, H. Thatoi, Characterization and evaluation of antibacterial activities of chemically synthesized iron oxide nanoparticles, World. J. Nano Sci. Eng., 2 (2012) 196.

[22] M.A. de Velasquez, T. Orta, I. Yáñez-noguez, B. Jiménez-cisneros, V.M. Luna Pabello, Adding silver and copper to hydrogen peroxide and peracetic acid in the disinfection of an advanced primary treatment effluent, Environ. Technol., 29 (2008) 1209–1217.

[23] W.E. Federation, A.P.H. Standard Methods for the Examination of Water and Wastewater, Association, Am. Public. Health. Assoc. (APHA), Washington, DC, USA, 2005.

[24] M. Tang, S. Zhang, X. Li, X. Pang, H. Qiu, Fabrication of magnetically recyclable Fe_3O_4@ Cu nanocomposites with high catalytic performance for the reduction of organic dyes and 4-nitrophenol, Mater. Chem. Phys., 148 (2014) 639.

[25] V. Rodríguez-González, R.B. Domínguez-Espíndola, S. Casas-Flores, O.A. Patrón-Soberano, R. Camposeco-Solis, S.W. Lee, Antifungal nanocomposites inspired by titanate nanotubes for complete inactivation of *Botrytis cinerea* isolated from tomato infection, ACS Appl. Mater. Interfaces, 8 (2016) 31625–31637.

[26] R.J. Watts, S. Kong, M.P. Orr, G.C. Miller, B.E. Henry, Photocatalytic inactivation of coliform bacteria and viruses in secondary wastewater effluent, Water. Res., 29 (1995) 95–100.

[27] E. Zhang, F. Li, H. Wang, J. Liu, C. Wang, M. Li, K. Yang, A new antibacterial titanium–copper sintered alloy: preparation and antibacterial property, Mater. Sci. Eng., C, 33 (2013) 4280.

[28] S. Pepper, M. Borkowski, M. Richmann, D. Reed, Determination of ferrous and ferric iron in aqueous biological solutions, Anal. Chim. Acta, 663 (2010) 172.

[29] Y.-S.E. Lin, R.D. Vidic, J.E. Stout, L.Y. Victor, Individual and combined effects of copper and silver ions on inactivation of *Legionella pneumophila*, Water Res., 30 (1996) 1905.

[30] S.B. Somani, N.W. Ingole, Formulation of kinetic model to predict disinfection of water by using natural herbs, Int. J. Environ. Sci., 2 (2012) 1344.

[31] J.C. Crittenden, R.R. Trussell, D.W. Hand, K.J. Howe, G. Tchobanoglous, MWH's Water Treatment: Principles and Design, John Wiley & Sons, Chichester, 2012.

[32] A. Mohseni-Bandpi, B. Kakavandi, R.R. Kalantary, A. Azari, A. Keramati, Development of a novel magnetite–chitosan composite for the removal of fluoride from drinking water: adsorption modeling and optimization, RSC Adv., 5 (2015) 73279.

[33] R.R. Kalantary, A. Azari, A. Esrafili, K. Yaghmaeian, M. Moradi, K. Sharafi, The survey of Malathion removal using magnetic graphene oxide nanocomposite as a novel adsorbent: thermodynamics, isotherms, and kinetic study, Desal. Wat. Treat., 57 (2016) 28460–28473.

[34] M. Raffi, S. Mehrwan, T.M. Bhatti, J.I. Akhter, A. Hameed, W. Yawar, M.M. ul Hasan, Investigations into the antibacterial behavior of copper nanoparticles against *Escherichia coli*, Ann. Microbiol., 60 (2010) 75–80.

[35] J.R. Conway, A.S. Adeleye, J. Gardea-Torresdey, A.A. Keller, Aggregation, dissolution, and transformation of copper nanoparticles in natural waters, Environ. Sci. Technol., 49 (2015) 2749.

[36] J.A. Lemire, J.J. Harrison, R.J. Turner, Antimicrobial activity of metals: mechanisms, molecular targets and applications, Nat. Rev. Microbiol., 11 (2013) 371.

[37] K.S. Chaturvedi, J.P. Henderson, Pathogenic adaptations to host-derived antibacterial copper, Front. Cell. Infect. Microbiol., 4 (2014) 3.

[38] M. Shi, H.S. Kwon, Z. Peng, A. Elder, H. Yang, Effects of surface chemistry on the generation of reactive oxygen species by copper nanoparticles, ACS Nano, 6 (2012) 2157.

[39] M. Monachese, J.P. Burton, G. Reid, Bioremediation and tolerance of humans to heavy metals through microbial processes: a potential role for probiotics? Appl. Environ. Microbiol., 78 (2012) 6397.

[40] M. Moradi, R.R. Kalantary, A. Esrafili, A.J. Jafari, M. Gholami, Visible light photocatalytic inactivation of *Escherichia coli* by natural pyrite assisted by oxalate at neutral pH, J. Mol. Liq., 248 (2017) 880.

[41] V. Ochoa-Herrera, G. León, Q. Banihani, J.A. Field, R. Sierra-Alvarez, Toxicity of copper (II) ions to microorganisms in biological wastewater treatment systems, Sci. Total Environ., 412 (2011) 380.

[42] M.J. Domek, M.W. Lechevallier, S.C. Cameron, G.A. McFeters, Evidence for the role of copper in the injury process of coliform bacteria in drinking water, Appl. Environ. Microbiol., 48 (1984) 289.

[43] Z. Hu, K. Chandran, D. Grasso, B.F. Smets, Comparison of nitrification inhibition by metals in batch and continuous flow reactors, Water Res., 38 (2004) 3949–3959.

[44] Y. Kurmaç, The impact of toxicity of metals on the activity of ureolytic mixed culture during the precipitation of calcium, J. Hazard. Mater., 163 (2009) 1063.

[45] C. Matocha, A. Karathanasis, S. Rakshit, K. Wagner, Reduction of copper (II) by iron (II), J. Environ. Qual., 34 (2005) 1539.

[46] M. Valko, H. Morris, M. Cronin, Toxicity and oxidative stress, Curr. Med. Chem., 12 (2005) 1161.

[47] S.P. Pathak, K. Gopal, Evaluation of bactericidal efficacy of silver ions on *Escherichia coli* for drinking water disinfection, Environ. Sci. Pollut. Res. Int., 19 (2012) 2285.

[48] Y.H. Kim, R. Hensley, Effective control of chlorination and dechlorination at wastewater treatment plants using redox potential, Water Environ. Res., 69 (1997) 1008–1014.

[49] I. De la Rosa-Gómez, M.T. Olguín, D. Alcántara, Bactericides of coliform microorganisms from wastewater using silver-clinoptilolite rich tuffs, Appl. Clay Sci., 40 (2008) 45–53.

[50] M.I. Sáez, J.J. Casas, J.L. Guil-Gerrero, M.D. Gil, R. Cañero, M.D. Suárez, Effects of organic matter, alkalinity and pH on acute copper toxicity to mosquitofish, *Gambusia holbrooki*: implications for a multipurpose management of irrigation ponds, Int. Rev. Hydrobiol., 98 (2013) 262.

[51] M.Y. Pamukoglu, F. Kargi, Copper (II) ion toxicity in activated sludge processes as function of operating parameters, Enzyme Microb. Technol., 40 (2007) 1228.

[52] D. Zeynalzadeh, R. Rezaei Kalantary, R. Nabizadeh Nodehi, A. Esrafili, M. Alimohamadi, A. Mokammel, Comparing efficiency of magnetic silver nanoparticles and magnetic silver nanoparticles modified with carbon layer on municipal wastewater disinfection, J. Health, 6 (2015) 7.

[53] K.J. Kramer, R.G. Jak, B. van Hattum, R.N. Hooftman, J.J. Zwolsman, Copper toxicity in relation to surface water-dissolved organic matter: biological effects to *Daphnia magna*, Environ. Toxicol. Chem., 23 (2004) 2971.

[54] V. Luna-Pabello, M.M. Rios, B. Jimenez, M. Orta De Velasquez, Effectiveness of the use of Ag, Cu and PAA to disinfect municipal wastewater, Environ. Technol., 30 (2009) 129.

[55] H.R. Daly, I.C. Campbell, B.T. Hart, Copper toxicity to *Paratya australiensis*: II. Influence of bicarbonate and ionic strength, Environ. Toxicol. Chem., 9 (1990) 1007.

[56] A. Sheikhmohammadi, S.M. Mohseni, M. Sardar, M. Abtahi, S. Mahdavi, H. Keramati, Z. Dahaghin, S. Rezaei, M. Almasian, M. Sarkhosh, M. Faraji, Application of graphene oxide modified with 8-hydroxyquinoline for the adsorption of Cr (VI) from wastewater: optimization, kinetic, thermodynamic and equilibrium studies, J. Mol. Liq., 233 (2017) 75–88.

[57] D.J. Naghan, A. Azari, N. Mirzaei, A. Velayati, F.A. Tapouk, S. Adabi, M. Pirsaheb, K. Sharafi, Parameters effecting on photocatalytic degradation of the phenol from aqueous solutions in the presence of ZnO nanocatalyst under irradiation of UV-C light, Bulg. Chem. Commun., 47 (2015) 8–14.

[58] L.-F. Wang, N. Habibul, D.-Q. He, W.-W. Li, X. Zhang, H. Jiang, H.-Q. Yu, Copper release from copper nanoparticles in the presence of natural organic matter, Water Res., 68 (2015) 12.

[59] J.D. Cuppett, S.E. Duncan, A.M. Dietrich, Evaluation of copper speciation and water quality factors that affect aqueous copper tasting response, Chem. Senses, 31 (2006) 689.